

# PERFORMANCE ANALYSIS of PEMFC for LONG ENDURANCE HYBRID POWERED UNMANNED AERIAL VEHICLE

Zehra URAL BAYRAK<sup>1</sup>, Ufuk KAYA<sup>2</sup>, Eyyup OKSUZTEPE<sup>3</sup>  
<sup>1,2,3</sup>Firat University, School of Aviation, Department of Avionics, 23180, Elazig, Turkey  
Corresponding author: Zehra URAL BAYRAK, e-mail: zural@firat.edu.tr

## REFERENCE NO

FCEL-06

### Keywords:

UAV, PEMFC, PMSM, hybrid, long endurance

## ABSTRACT

In this study, the endurance of fuel cell (FC) and FC with batteries are investigated for cruise phase of unmanned aerial vehicle (UAV). A proton exchange membrane (PEM) FC is chosen because of its energy efficiency and low operating temperature. The selected batteries are Lithium-Ion (Li-ion) and Nickel Metal Hydride (Ni-MH) due to commonly usage in aerial applications. The FC and batteries have same energy capacities with different characterizations. It has been observed that the model with only FC has the longest endurance for the cruise phase. The flight time changes for different battery-fuel cell combinations because of varying total weight and characterization of the system. The linearized models of the UAV are simulated in MATLAB/Simulink for cruise phase.

## 1. INTRODUCTION

Recently, carbon based fuels are widely using for combustion engines in aviation. Although their high power densities, these fuels produce carbon emissions environmentally hazardous. Conversely, electrical power sources are more environment-friendly energy technologies. In aviation, mostly used electrical sources are fuel cells, solar cells, batteries, ultra-capacitors, etc.

Electrical powered UAVs are operated by batteries, generally. Due to lack of mass and volume in aviation, there are some limitations on battery usage. For this reason, power sources with higher energy densities are needed. There are different alternative energy sources in the literature for increasing flight time [1-6]. In these studies, they used varied energy sources scenarios such as solar/hydrogen systems, batteries, ultra-capacitors/fuel cells, fuel cell/gas turbine hybrid systems, etc. The batteries also chosen to provide a peak power enough for take-off, climb and other power demanding maneuvers, even transients. The fuel cell system provided enough cruise power for longer endurance flights. Using a combination of Lithium Ion Polymer batteries (LiPo) and a PEMFC as the energy sources of the UAV helps to achieve a good compromise amongst high specific energy, high specific power and low weight.

When compared with other storage systems,

especially lithium-based batteries, fuel cell systems have the highest energy-to-weight ratio presented in Fig. 1.

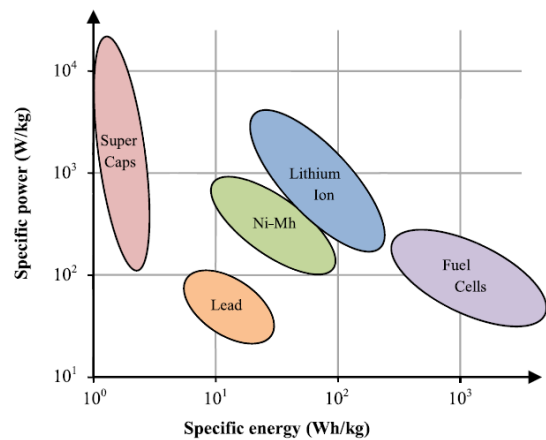


Fig. 1. Specific energy and power of different storage technologies [1]

The PEMFC is adopted in this study that require rapid start-up and quick response to load change like low power required applications. Also, it is silent without any moving parts, has long operating life, and is more efficient than internal combustion engines [7-10].

## 2. MODELING of HYBRID POWERED UNMANNED AERIAL VEHICLE

The UAV model consists of a PEMFC, a battery, DC/DC converter, permanent magnet synchronous motor (PMSM) driver and

PMSM. The Li-ion and Ni-MH batteries are chosen due to commonly using for the UAVs. Power sources are connected to the DC/DC converter via switches shown in Fig. 2. The switches represent power source selections. The bi-directional DC/DC buck-boost converter is used for voltage regulation and increasing energy efficiency. The propulsion source of the UAV is PMSM driven by PMSM driver.

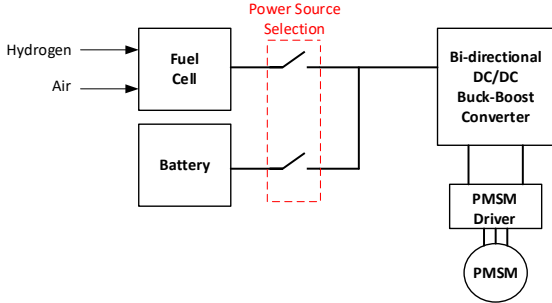


Fig. 2. General block diagram of the hybrid UAV model.

There are three different cases for proposed UAV model. FC, FC with Li-ion and FC with Ni-MH are used in scenarios 1, 2, 3, respectively. The scenarios are given in Table 1 depending on usage of these power sources.

Table 1. Power sources usage scenario

Scenario	FC	Li-ion Battery	Ni-MH Battery
1	✓		
2	✓	✓	
3	✓		✓

## 2.1. The Linearized UAV Model

The endurance of the UAV is related with total power consumption of the propulsion source. The PMSM propulsion source of the UAV is empowered by fuel cell/battery hybrid power source. There are several flight phases during UAV operation. Therefore, the total load on the propulsion source varies with time and effects the power consumption. For efficiency analysis, the power consumption of the PMSM must be unraveled. The power consumption of the PMSM depends on four major forces on the UAV: thrust, lift, drag and weight. In Fig. 3 those forces are shown on an UAV model.

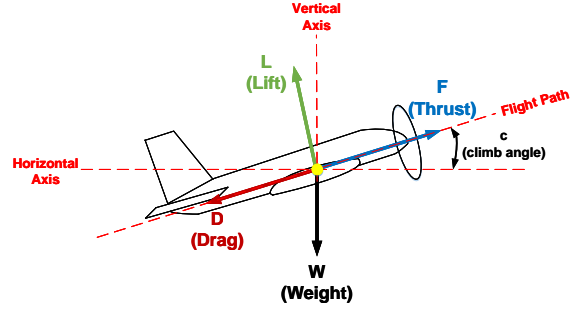


Fig. 3. The major forces on an UAV model

General flight equations can be given as Eq.1 for vertical plane and Eq.2 for horizontal plane.

$$F \cdot \sin(\phi) - D \cdot \sin(\phi) + L \cdot \cos(\phi) - W = m \cdot a_v \quad (1)$$

$$F \cdot \cos(\phi) - D \cdot \cos(\phi) - L \cdot \sin(\phi) - W = m \cdot a_h \quad (2)$$

where  $F$  is thrust,  $D$  is drag,  $W$  is the total weight of the UAV,  $L$  is lift,  $\phi$  is the climb angle,  $m$  is the total mass,  $a_v$  is vertical acceleration and  $a_h$  is horizontal acceleration. It is accepted that the total mass is homogeneous.

The  $\phi$  varies for different phases of flight changes the forces, which are given in Eq.1 and Eq.2. Cruise is the only considered flight phase in this study because of complexity of these changes. Lift is given in Eq.3.

$$L = \frac{c}{3} \cdot \rho \cdot \omega^2 \cdot \frac{r^3}{3} \cdot \sin(\theta) \quad (3)$$

where  $c$  is the width of the propeller blade,  $\rho$  is the air density,  $\omega$  is the rotational speed of the propeller,  $r$  is the radius of the propeller,  $\theta$  is the angle of the propeller blade. Required torque ( $T$ ) for cruise phase is given in Eq.4.

$$T = \frac{(3 \cdot m \cdot g)}{4} \cdot \left[ \frac{(1 - \cos(\theta))}{\sin(\theta)} \right] \cdot r \quad (4)$$

where  $g$  is the gravitational acceleration.

$$V = \sqrt{\frac{L}{A \cdot C_l} \cdot \frac{2}{\rho}} \quad (5)$$

In Eq. 5,  $V$  is velocity of the UAV,  $A$  is the reference area of the UAV,  $C_l$  is the lift coefficient. The constants used for the proposed UAV model are listed Table.2.

Table 2. The constants for the linearized model of the UAV

Symbol	Parameter	Value	Unit
$m$	The total mass of the UAV without power Sources	3.6	kg
$g$	The gravitational acceleration	9.8	m/s <sup>2</sup>
$\rho$	The density of air	1.225	kg/m <sup>3</sup>
$C_d$	The drag coefficient	0.077	-
$C_l$	The lift coefficient	1.163	-
$A$	The reference area of UAV	0.9	m <sup>2</sup>
$d$	The propeller diameter	0.533	m
$V$	The maximum velocity of UAV	25	m/s
$p$	Propeller pitch	0.330	m
$m_p$	Propeller weight	0.04	kg
$c$	Width of the propeller blade	0.050	m
$\theta$	Angle of the propeller blade	0.194	rad

The aerodynamic specifications of the UAV has determined according to selected airfoil FX 76-MP-120.

## 2.2. Fuel Cell

A fuel cell is an energy converter that generates electrical energy via electrochemical reactions. The FC uses hydrogen as a fuel and generates electric without intermediate stages. The FC can run indefinitely as long as hydrogen and air are supplied. The most commonly used of the fuel cells is PEMFC because of low operating temperature, high current density, cost and weight, compact volume; longer stack life; and rapid start-ups. The PEMFC is used as the proposed system's primary electric source. A PEMFC stack has four main units, which are anode, cathode, electrolyte layer and the gas flow channels.

Membrane is sandwiched between two catalyzed electrodes (anode and cathode) in a PEMFC. Firstly, the hydrogen is pressurized and provided to the anode. Then the hydrogen is split into electrons and protons at the anode catalytic layer. It is flowing through an electrolytic membrane, which blocks the electrons from travelling to the catalytic layer of the cathode. Finally, the electrons travel through an external circuit to the cathode. Electric current is generated in this stage.

The mathematical models are used to obtain the characteristics of the FC stack, and the polarization curve is obtained by evaluating the developed mathematical model of the PEMFC stack in Matlab/Simulink. Inputs of the FC model are partial pressures of hydrogen, oxygen and steam and current density of the fuel cell stack.

The cell voltage ( $V_{cell}$ ) can be determined in any conditions by using Eq.6. When a cell operates with a load,  $E$  (no load voltage) decreases with the increment of the voltages defined as  $V_{act}$  (activation overvoltage),  $V_{ohm}$  (ohmic overvoltage) and  $V_{conc}$  (concentrate overvoltage).

$$V_{cell} = E - V_{act} - V_{ohm} - V_{conc} \quad (6)$$

Cell voltage ( $V_{cell}$ ) can be solved as a function of cell temperature, reactant pressure and membrane hydration. Detailed model equations are given in reference 11. If all of cells are connected in series, stack voltage ( $V_{stack}$ ) is obtained from the multiplication of cell voltage and cell number. It is given in Eq.7. [11]

$$V_{stack} = V_{cell} \cdot N \quad (7)$$

The fuel cell properties are chosen by Horizon Energy Systems' AEROPAK. AEROPAK is PEMFC designed for aerial applications. It has light weight, small size and good hydrogen capacity with enough performance for UAVs. Some of the features of AEROPAK are shown in Table 3.

Table 3. Characteristics of AEROPAK fuel cell

<b>Continuous output power</b>	200 W
<b>Continuous current</b>	10 Amps
<b>Output voltage range</b>	20-32 V
<b>Mass</b>	0.470 kg
<b>Lifetime at rated power</b>	500h
<b>Operating temperature</b>	0-40 °C
<b>Weight</b>	400 g

### 2.3. Battery

Li-ion and Ni-MH batteries are the most commonly used types of battery for aerial applications. They have their own advantages and disadvantages.

The Li-ion batteries can hold the charge for long time and can stay charged in storage. Also, they are lighter than other types of batteries for same capacity. Li-ion battery chemistry delivers a high open-circuit voltage. Also, they have low self-discharge rate and reduced toxicity. They don't suffer from battery memory effect. On the other hand, the performance of Li-ion batteries can dramatically affect by materials that used for anode and cathode. They are not available in all sizes. They need different chargers for different batteries.

The Ni-MH batteries cost effective comparing Li-ion batteries. They are available in different sizes and they can operate in low voltages. They run at full strength for life of the charge. Also, the voltage of Ni-MH batteries does not falter like most rechargeable batteries and stays at a constant voltage regardless of the remaining charge level. However, they lose charge in storage and deplete voltage over time. They are needed to charge before usage. This is not convenient for sudden usage situations. Hence, they should use with proper charging and storing system for effectiveness.

In our study, Ni-MH and Li-ion batteries are chosen. Ni-MH has 218-gram weight, 8500mAh capacity and Li-ion has 300-gram weight, 8500mAh capacity.

### 2.4. Bi-directional DC/DC Buck-Boost Converter

For long endurance flight, the power sources have higher energy capacities are needed. Mostly, when the stored energy capacity of

power source increases, mass and volume of the power source increases too. However, due to lacks of weight and space in aviation some size reductions must be done for the power source. After these reductions the power capacity of power sources reduces. Also, the fuel cell produces lower voltage than the PMSM needs for same reason. Therefore, a DC/DC buck-boost converter is needed.

The buck-boost converter provides required output DC voltage by decreasing or increasing input voltage. On the other hand, the bi-directional DC/DC buck-boost converter has the advantage of working bi-directionally. During the motor braking operation, this feature let us to charge battery with the energy produced by back electromotive force (emf) of PMSM. Also, this advantage increases energy efficiency of the system. The basic circuit scheme of bi-directional DC/DC buck-boost cascade converter is given in Fig. 4 [13]. In this figure, S1, S2, S3 and S4 represent switches. Also D1, D2, D3 and D4 represent diodes. C1 and C2 represent capacitors.

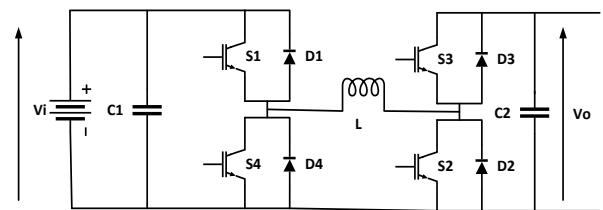


Fig. 4. Bi-directional buck-boost cascade converter scheme

The bi-directional buck-boost cascade converter can operate four different modes for motoring and braking operations.

- Motoring step-down (buck) mode
- Motoring step-up (boost) mode
- Braking step-down (buck) mode
- Braking step-up (boost) mode

### 2.5. The Propulsion: PMSM

The electrical motor is the propulsion source of the UAV. There are several types of electrical motors for aerial applications. Brushless DC motor (BLDC) and permanent magnet synchronous motor (PMSM) are most commonly used types of motor in aviation.

Each of them has their own advantages and disadvantages. The PMSM has higher efficiency and higher torque when comparing BLDC. Also it is a brushless electrical motor as BLDC. However, it has higher cost and is more complex to control. There isn't any copper loss on rotor. It requires low maintenance. It has simple structure and is easy to produce.

PMSMs consist of two main units as other types of electrical motors: stator and rotor. Distinctly, PMSMs use permanent magnets producing air gap magnetic fields. There is no need any magnetizing component of stator current due to permanent magnets. In order to use PMSM in the UAV model, the mathematical equations of PMSM is needed. These equations are given in Eq.8, Eq.9, Eq.10, Eq.11 and Eq.12.

$$u_{sd} = R_s \cdot i_{sd} + \frac{d}{dt} \cdot \Psi_{sd} - \omega_r \cdot \Psi_{sq} \quad (8)$$

$$u_{sq} = R_s \cdot i_{sq} + \frac{d}{dt} \cdot \Psi_{sq} + \omega_r \cdot \Psi_{sd} \quad (9)$$

$$\Psi_{sd} = L_{sd} \cdot i_{sd} + \Psi_M \quad (10)$$

$$\Psi_{sq} = L_{sq} \cdot i_{sq} \quad (11)$$

$$T_e = \frac{3}{2} \cdot p \cdot (\Psi_{sd} \cdot i_{sq} - \Psi_{sq} \cdot i_{sd}) \quad (12)$$

where  $\Psi_{sd}$  is the d-axis stator magnetic flux,  $\Psi_{sq}$  is the q-axis stator magnetic flux,  $\Psi_M$  is the rotor magnetic flux,  $L_{sd}$  is the d-axis stator leakage inductance,  $L_{sq}$  is the q-axis stator leakage inductance,  $i_s$  is the stator current,  $R_s$  is the stator winding resistance,  $T_e$  is the electromagnetic torque and  $p$  is the double pole number.

There are two vector control methods for PMSM: Field oriented control method (FOCM) and direct torque control method (DTCM). The position and speed sensors are required for reliable rotor control in both control methods. However, the performance of DTCM is better. The mathematical simplicity of DTCM makes it possible to use high sampling frequencies. Contrary, DTCM shows poor performance in steady-state due to

high ripple levels in stator current, torque and flux linkage. In a study [14], researchers studied on ripple reduction in PMSMs.

### 3. SIMULATION and RESULTS

Proposed linearized UAV model is simulated in Mathworks MATLAB/Simulink. Block diagram of the model is represented in Fig. 5.

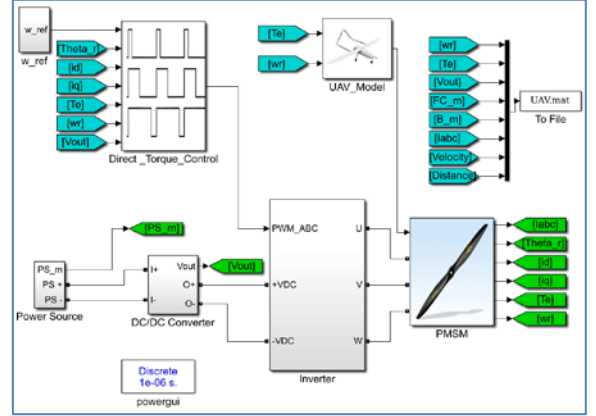


Fig. 5. Simulink block diagram of the system

Three different scenarios are considered according to power source usage in our simulation. FC, FC with Li-ion, FC with Ni-MH are powered the UAV in scenario 1, 2, 3, respectively. Total endurance, distance and weight are listed in Table 4 for these scenarios.

Table 4. Utmost values of the total flight

Scenario	Endurance (h)	Total distance (km)	Total weight (kg)
1	0.994	19.717	4
2	0.989	19.606	4.018
3	0.960	19.046	4.1

The velocity of the UAV is 5.5 m/s and the average propeller speed is 2369 rpm. These values don't change for three scenarios. Also the total energy is selected 200 Wh. In scenario 2 and 3, FC with batteries energies are selected 100 Wh for each power sources. Total simulation time is determined by energy consumption.

The total mass and characteristics of the power sources effects endurance. Total mass which, correlated with required torque, is inversely proportional with endurance. In spite of that, total energy of the UAV is same

for three scenarios. For this reason, endurance will be different which is revealed in Fig. 6.

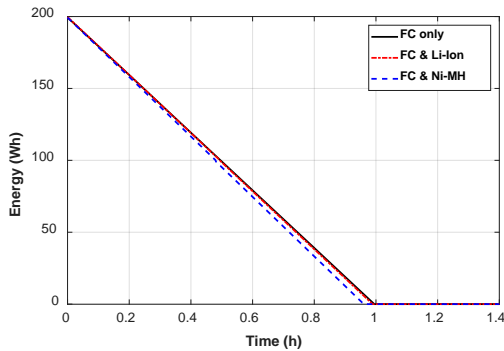


Fig. 6. Energy consumption

The velocity calculated by Eq.5. does not change over time in cruise phase. Fig. 7 demonstrates this case.

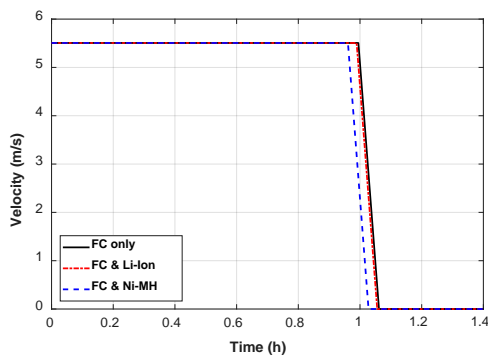


Fig. 7. The velocity of the UAV

The total distance of the UAV is shown in Fig. 8. Since the velocity is constant through the endurance, the total distance increases linearly over time. It will be different because of difference in flight times.

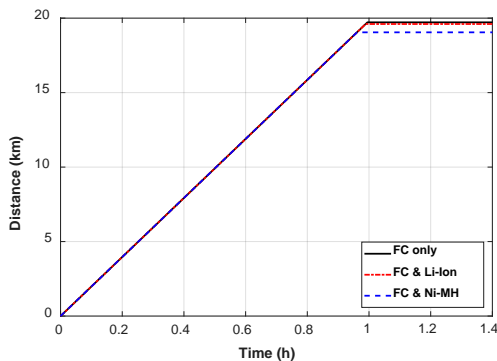


Fig. 8. The total distance travelled by the UAV

The reference speed of propeller is decided by required torque, which is related with F. In

Fig. 9, the speed controller adjusts the speed of the propeller to the reference speed during flight time. MULA simulati

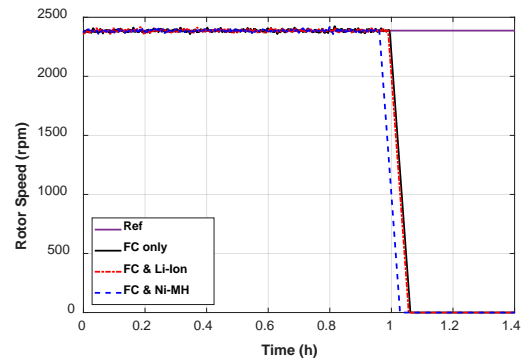


Fig. 9. Speed of the propeller

Because of the difficulties of simulating in real time, the simulation time has been extended with a calculated time coefficient.

#### 4. CONCLUSIONS

The model simulated in MATLAB/Simulink is linearized model of the UAV for cruise phase. Since the UAV travels at a constant speed in cruise phase, only total weight and characteristics of the power sources determine the total duration of the flight. When that is considered, the model with only FC has the longest endurance while FC with Ni-MH having the lowest endurance. The situation is exactly the opposite when we consider weight. So, FC with Ni-MH is the heaviest.

For power sources with same capacities, it is more advantageous to use the FC during the cruise phase. For the other flight phases, it will be more efficient to use the hybrid system. Because the energy generated by regenerative operation of the motor will be stored in the battery during landing phase.

#### References

- [1] N. Lapena-Rey, J.A. Blanco, E. Ferreyra, J.L. Lemus, S. Pereira, E. Serrot, A fuel cell powered unmanned aerial vehicle for low altitude surveillance missions, *International Journal of Hydrogen Energy*, 42, 2017, 6926-6940.
- [2] Byeong Gyu Gang, Hyuntak Kim, Sejin Kwon, Ground simulation of a hybrid power strategy using fuel cells and solar cells

for high-endurance unmanned aerial vehicles, *Energy*, 141, 2017, 1547-1554.

[3] P. Aguiar, D.J.L. Brett, N.P. Brandon, Solid oxide fuel cell/gas turbine hybrid system analysis for high-altitude long-endurance unmanned aerial vehicles, *International Journal of Hydrogen Energy*, 33, 2008, 7214-7223.

[4] J.Y. Hung, L.F.Gonzalez, On parallel hybrid-electric propulsion system for unmanned aerial vehicles, *Aerospace Sciences*, 51, 2012, 1-17.

[5] Romeli Barbosa, B. Escobar, Victor M. Sanchez, J. Hernandez, R. Acosta, Y. Verde, Sizing of a solar/hydrogen system for high altitude long endurance aircrafts, *International Journal of Hydrogen Energy*, 39, 2014, 16637-16645.

[6] Charles Chiang, Christopher Herwerth, Dr.Maj Mirmirani, Alan Ko, Shigeru Matsuyama, Sang Bum Choi, Natthawit Nomnawee, Systems Integration of a Hybrid PEM Fuel Cell/Battery Powered Endurance UAV, 46th AIAA Aerospace Sciences Meeting and Exhibit, Reno, Nevada, 7 - 10 January 2008.

[7] Cheolnam Yang, Sungmo Moon, Yangdo Kim, A fuel cell/battery hybrid power system for an unmanned aerial vehicle, *Journal of Mechanical Science and Technology*, 30, 5, 2016, 2379-2385.

[8] Daming Zhou, Alexandre Ravey, Ahmed Al-Durra, Fei Gao, A comparative study of extremum seeking methods applied to online energy management strategy of fuel cell hybrid electric vehicles, *Energy Conversion and Management*, 151, 2017, 778-790.

[9] Mohamed Gadalla, Sayem Zafar, Analysis of a hydrogen fuel cell-PV power system for small UAV, *International Journal of Hydrogen Energy*, 41, 2016, 6422-6432.

[10] Chung-Neng Huang, Yui-Sung Chen, Design of magnetic flywheel control for performance improvement of fuel cells used in vehicles, *Energy*, 118, 2017, 840-852.

[11] Ufuk Kaya, Zehra Ural Bayrak, Eyyup Oksuztepe, Fuel cell/battery hybrid powered unmanned aerial vehicle with permanent magnet synchronous motor, *International*

*Journal of Sustainable Aviation*, 3, 2, 2017, 130 – 150.

[12] Lieh, J., Spahr, E., Behbahani, A., Hoying, J., Design of hybrid propulsion systems for unmanned aerial vehicles, Proceedings of the 17th AIAA International Space Planes and Hypersonic Systems and Technologies Conference, San Francisco, California, 11–14 April 2011.

[13] Caricchi, F., Crescimbin, F., Capponi, F.G. and Solero, L., Study of bi-directional buckboost converter topologies for application in electrical vehicle motor drives, Proceedings of the 13th Annual Applied Power Electronics Conference and Exposition (APEC'98), Anaheim, California, IEEE, 1, 287–293, 15–19 February 1998.

[14] Erken, F., Oksüztepe, E. and Kürüm, H., Online adaptive decision fusion based torque ripple reduction in permanent magnet synchronous motor, *IET Electric Power Applications*, 10, 3, 2016, 189-196.